

Advanced measurement techniques to characterize the near-specular reflectance of solar mirrors

Cite as: AIP Conference Proceedings **2126**, 110003 (2019); <https://doi.org/10.1063/1.5117618>
Published Online: 26 July 2019

Florian Sutter, Aránzazu Fernández-García, Anna Heimsath, Marco Montecchi, and Cristina Pelayo



View Online



Export Citation

ARTICLES YOU MAY BE INTERESTED IN

[Advanced cyclic accelerated aging testing of solar reflector materials](#)

AIP Conference Proceedings **2126**, 160007 (2019); <https://doi.org/10.1063/1.5117670>

[Durability testing of a newly developed hydrophilic anti-soiling coating for solar reflectors](#)

AIP Conference Proceedings **2126**, 160002 (2019); <https://doi.org/10.1063/1.5117665>

AIP | Conference Proceedings

Get **30% off** all
print proceedings!

Enter Promotion Code **PDF30** at checkout



Advanced Measurement Techniques to Characterize the Near-Specular Reflectance of Solar Mirrors

Florian Sutter^{1, a)}, Aránzazu Fernández-García², Anna Heimsath³, Marco Montecchi⁴, Cristina Pelayo⁵

¹DLR, Plataforma Solar de Almería, Senes Road, Km. 4.5, P.O. Box 44, E04200 Tabernas, Spain

²CIEMAT-Plataforma Solar de Almería, Senes Road, Km. 4.5, P.O. Box 22, E04200 Tabernas, Spain

³Fraunhofer-Institut für Solare Energiesysteme ISE, Heidenhofstr. 2, 79110 Freiburg, Germany

⁴ENEA C.R. Casaccia, Via Anguillarese, 301, 00123 S. Maria di Galeria, Roma, Italy

⁵Universidad de Zaragoza, Department of Applied Physics, Maria de Luna 3, 50018 Zaragoza, Spain

^{a)}Corresponding author: florian.sutter@dlr.de

Abstract. The precise measurement of the reflected energy from a solar reflector to the receiver is a challenging task because of its dependency on three different parameters: the wavelength of the incident light, its incidence angle and the acceptance angle of the receiver. Up to today, the commonly employed measurement equipment is not able to fully characterize the mirrors in the required range of parameters which is relevant for CSP. Within this work, four reflectometers were upgraded to overcome the current drawbacks. A Round Robin test among the different characterization methods has been carried out on four reflector materials. The conclusions drawn from the comparison of the measurement results help to improve the current SolarPACES Reflectance Guideline.

INTRODUCTION

The difficulty in measuring solar reflectance lies in the broad parameter range influencing the reflectance of a mirror employed in CSP. For instance, the wavelength of solar radiation lies in the range of $\lambda=[280-4000]\text{nm}$. To facilitate the measurement, the irradiance in the UV [280-320] and far IR (2500-4000] is neglected. This is reasonable since their weight in the total spectrum is 0.09 and 0.87% respectively. The incidence angles θ_i vary from near-normal up to $\theta_i=80^\circ$ in CSP plants [1]. The acceptance angle of the receiver φ_r defines the cone in which reflected rays from the mirror are intercepted by the receiver. The beam-spread of the reflected radiation is the angular radius of the sun $\varphi_s=4.7\text{mrad}$, augmented by an amount due to scattering, tracking or shape inaccuracies: $\varphi_r=\varphi_s+\varphi+\varphi_t+\varphi_p$ [2]. As indicated in [1], φ_r may lie in the range of $\varphi_r=[6-46]\text{mrad}$ for the Ivanpah solar tower, depending on the distance of the heliostat from the receiver. For parabolic trough collectors of EuroTrough geometry φ_r ranges from [12-20]mrad, depending on the distance of the incident ray from the vertex of the parabola.

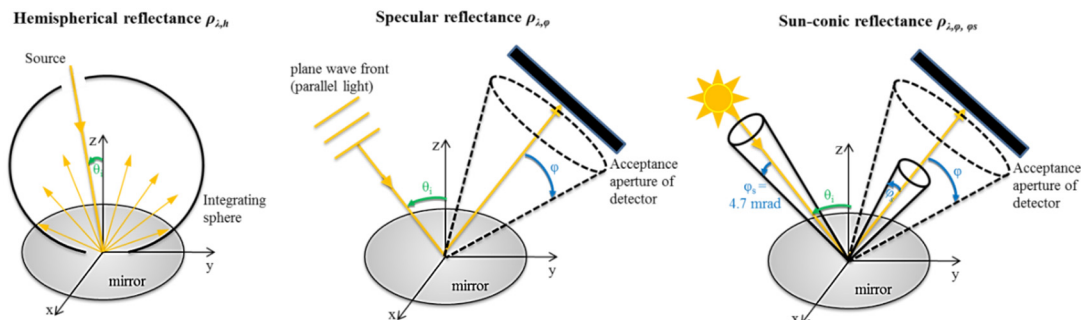


FIGURE 1. Reflectance parameters to describe solar mirrors

Tracking and shape inaccuracies of the mirror are considered separately from its losses caused by scattering, which are described by the specular reflectance. It is defined as the reflected light coming from perfectly parallel light (beam divergence of the light source is 0 mrad) into a cone angle of φ (see FIGURE 1, middle). Although φ as low as 1-2 mrad are relevant for solar towers, the measurement of specular reflectance at narrow acceptance angles of $\varphi < 7$ mrad is still very challenging. The reason is that the measurement beam of any reflectometer is obtained by a source whose geometrical dimension is extended and not punctual; that causes the beam divergence. A simple solution is to measure sun-conic reflectance as proposed in [3], for which the beam divergence of the light source is adapted to $\varphi_s = 4.7$ mrad, matching the sun disk viewed from the earth on a clear sky day (see FIGURE 1, right).

The actual SolarPACES Reflectance Guideline [4] provides a tool to obtain comparable reflectance measurements. However, the method has significant drawbacks, mainly due to the lack of current measurement equipment. On one hand, spectral measurements in the relevant wavelength range of $\lambda = [320-2500]$ nm are only carried out hemispherically using integrating spheres (see FIGURE 1, left). Specular reflectance measurements are only carried out monochromatically and without taking into account the beam divergence of the light source. Stable measurements can only be obtained down to $\varphi = 7.5$ mrad. Although commercial equipment exists, measuring as low as $\varphi = 2.3$ mrad, the authors' experience with these devices is that calibration procedures are tedious and reproducibility of the measurements is poor. On the other hand, reflectance is only measured at near normal incidence angles θ_i despite the fact that the most frequent θ_i in the solar field is considerably larger (e.g. the most frequent θ_i is 30° for a heliostat north-field and $\theta_i = 35^\circ$ for parabolic-trough, both positioned at $37^\circ 05'$ latitude [2]).

Missing data over the relevant λ -, θ_i - and φ -ranges for CSP may lead to inaccurate estimations of the reflected solar energy towards the receiver. In order to minimize the knowledge gap, research institutes have developed prototype lab-reflectometers. More recently, SolarPACES has approved a new project, financing some upgrading of those prototypes. The following section describes the measurement principle of four developed devices.

DEVELOPMENT OF EQUIPMENT TO MEASURE NEAR-SPECULAR REFLECTANCE

Spectral Specular Reflectometer (S2R) by DLR/CIEMAT

DLR/CIEMAT's Spectral Specular Reflectance Accessory (S2R) uses fiber optics to measure near-specular reflectance with the aid of an integrating sphere within the Perkin Elmer Lambda 1050 spectrophotometer [5]. The S2R is based on the commercially available General Purpose Optical Bench (PELA1003) from Perkin Elmer equipped with a 60 mm integrating sphere containing two detectors: a photomultiplier tube (PMT) for UV/VIS spectral measurements and an InGaAs photodiode detector for NIR applications, allowing to carry out measurements in the complete wavelength range of interest, $\lambda = [320-2500]$ nm. A suited specular light path (see FIGURE 2) has been implemented in order to measure sun-conic reflectance at variable φ and θ_i . The beam diversion of the system is $\varphi_s = 4.74$ mrad and the measurement spot is 22 mm in diameter. The sample is mounted on a rotating platform, allowing to adjust the incidence angle θ_i of the measurement in the range of $\theta_i = [10-70]^\circ$ by adjusting two micrometer screws. The acceptance angle φ of the measurement is defined by the diameter of the aperture placed in front of the integrating sphere. By turning the acceptance angle wheel $\varphi = 9.8; 12.3; 14.8; 20.2; 35.9; 107.4$ mrad can be realized.

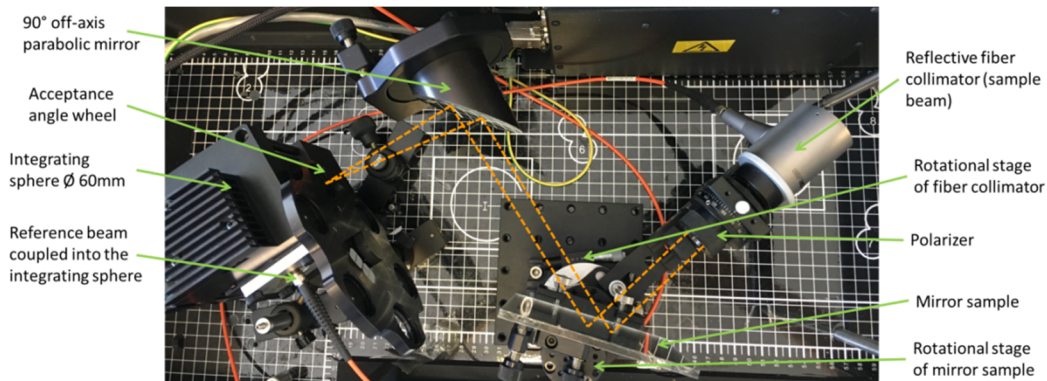


FIGURE 2. DLR/CIEMAT's S2R setup installed in PerkinElmer 1050. The beam path is indicated by the dashed lines.

The S2R was upgraded with the high performance polarizer crystal from PerkinElmer, operating in the range $\lambda=[300-2600]\text{nm}$, allowing to measure at different polarizations with the aim to improve accuracy at higher θ_i (see FIGURE 2). S- and p-polarized reflectance was measured for each incidence angle separately and finally the average of both measurements was computed to obtain the reflectance for a non-polarized light source like the sun.

In order to reduce error induced by fiber movement, the system was recalibrated for each incidence angle and polarization using a 1 mm silvered-glass reflector of known angular properties. The reference mirror was provided by ENEA and has been calibrated according to the Equivalent Model Algorithm (EMA) [6].

VLABS by Fraunhofer

Fraunhofer ISE's VLABS is a laboratory instrument to evaluate the bidirectional reflectance function and specular reflectance [8]. The upgraded VLABS-II system contains a white LED and filters for quasi-monochromatic light ($\pm 10\text{ nm}$ from the central wavelength). The light passes through a diffusor, variable pinholes and a lens-system before being received by a CCD array with high resolution and high quantum efficiency (see FIGURE 3 a and b).

The main characteristics of VLABS-II are:

- LED irradiation with blue, green and red light at $\lambda=450\text{ nm}$, $\lambda=550\text{ nm}$ and $\lambda=650\text{ nm}$ (wavelength range of white light source between 380nm- 780nm).
- Light source beam divergence half-angle of $\varphi_s=1\text{ mrad}$ or $\varphi_s=4.67\text{ mrad}$ for sun-conic reflectance measurements. Variable spot diameter on reflector samples between 0.6 mm to 10 mm.
- Variable incidence angles between $10^\circ < \theta_i < 80^\circ$
- Acceptance angles φ in the range of $[1-33]\text{mrad}$, with a resolution of 0.05mrad
- The dynamic range of the detector camera covers about five orders of magnitude
- Results are the angle resolved scatter, specular reflectance and sun-conic reflectance

For the calculation of the near-specular reflectance the deconvolution approach proposed in [7] was enhanced. This also allows the evaluation of the beam spread by an angle resolved scatter function. Additionally, the sun-conic reflectance can be measured directly at discrete wavelengths. Spectral behavior is modeled by applying the total integrated scatter (TIS) theory (see eq.3 and [9]).

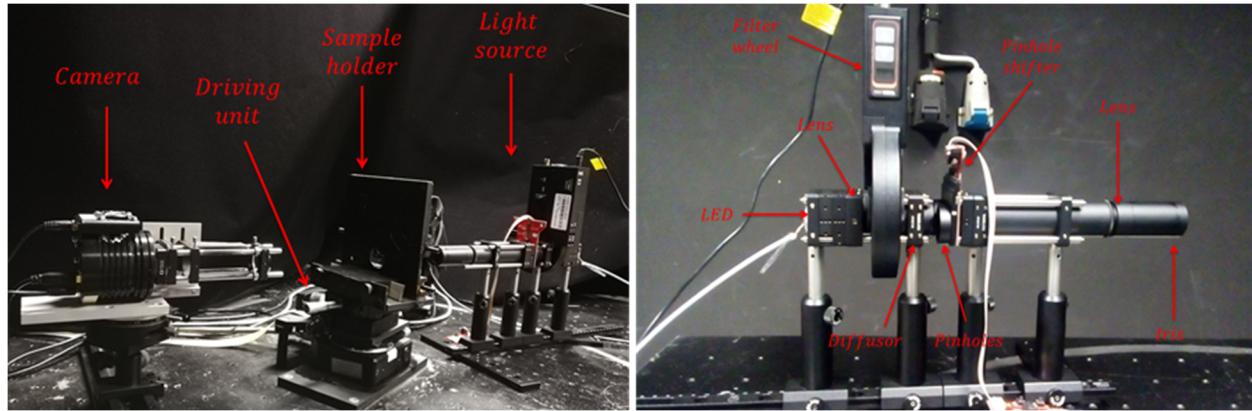


FIGURE 3. VLABS measurement set-up. a) complete set-up. b) light source

SMQ2 by ENEA

The ENEA strategy for evaluating off-normal near-specular solar-weighted reflectance is based on modeling the hemispherical spectral reflectance with EMA [6], and the ratio between near-specular and hemispherical reflectance with the Total Integrating Scattering (TIS) equation [7]. In the latter case, the roughness is replaced by the heuristic parameter σ_φ , non-physically depending on the acceptance angle. The SMQ experimental set-up was conceived for measuring the important parameter σ_φ without need of any deconvolution procedure by using laser beams with low divergence ($< 1\text{ mrad}$) and small diameter ($< 1\text{ mm}$). The first version of the instrument was presented in 2012 [6], followed closely by an upgraded version in 2013 [10]. Now, with the latest version SMQ2, shown in FIGURE 4a, the following improvements have been achieved: i) the coherent length of the measurement beam is similar to that

of common spectrophotometers thanks to the adoption of the supercontinuum white light laser SuperK Compact (SKC) by NKT Photonics; ii) the experimental set-up is greatly simplified, being near-specular reflectance evaluated by an image processing method and the lock-in amplifier directly triggered by the pulsed laser (no need of optical chopper); iii) the instrument is self-calibrating, scaling the digital image using the ratio of the two integrating sphere measurements, with open and closed exit port; iv) shorter measurement time; v) enhanced sensitivity, which makes also high specular mirrors fully measurable; vi) acceptance-angle range extended up to 50 mrad.

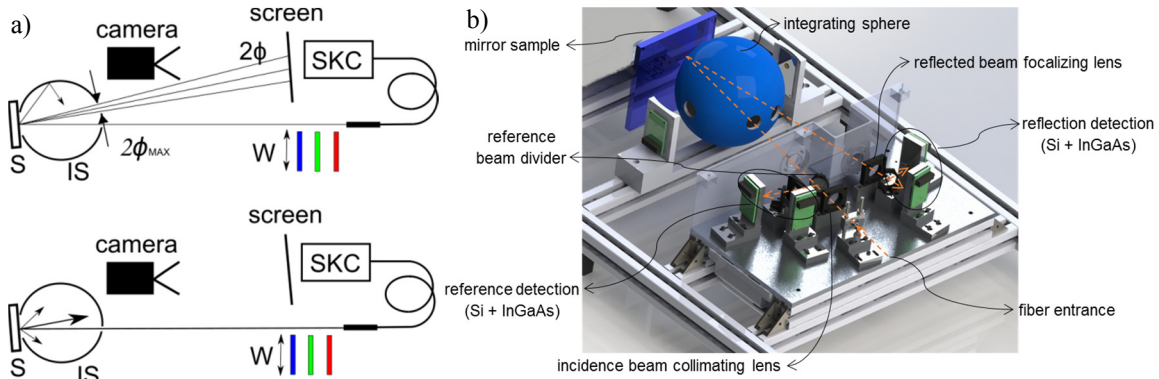


FIGURE 4. a) SMQ2, the latest version of the Solar Mirror Qualification set-up developed by ENEA. b) Experimental setup to measure hemispherical reflectance from UNIZA. The optical path is shown by the orange dashed lines.

Experimental Setup by University of Zaragoza

At the University of Zaragoza (UNIZA), the hemispherical reflectance is characterized by means of a laboratory spectrophotometer (Fig.4b), which can measure in the range of $\lambda=[320-2500]\text{nm}$, at fixed $\theta_i=8^\circ$. The light source is comprised of a combined xenon and halogen lamp. Their light is modulated using a mechanical chopper for synchronous detection. Detected signals are amplified with a digital lock-in to achieve a better signal to noise ratio. Wavelength selection is performed by a monochromator (Spectral Products model CM110) and a filter wheel that selects the appropriate interference filter to remove harmonic peaks from the diffraction gratings.

The incident beam leaves the monochromator and is directed to the sample through a 550 μm diameter multimodal optical fiber (Thorlabs reference M37L01). At the exit of the fiber, the light beam is collimated with a suitable lens of 50 mm focal length, so that the divergence of the beam impinging on the sample is comparable to that of the sun on earth surface (ϕ_s around 5 mrad). There is also a 10 mm diameter stop to control the size of the beam. A portion of this beam is diverted to a reference detection branch of the device, so it can monitor the fluctuations of the light source. The sample under test is placed after a 150 mm integrating sphere as shown in FIGURE 4b. The reflected beam exits the integrating sphere and is focused onto the detector element by means of a lens of 75 mm focal length. The detector element is a silicon photodiode for the 320-1050 nm range, and a thermoelectrically cooled InGaAs photodiode for the 1050-2500 nm range. Both are connected to their electronic preamplifiers with a software-controlled gain, and the pre-amplified signal is sent to the computer for a software-based lock-in treatment.

Near-specular reflectance is measured at UNIZA with a configurable laboratory setup, similar to the spectrophotometer described before, but devoid of the integrating sphere and fiber connections so that it can be more easily arranged to measure at 10, 30 and 60° incident angle and fixed acceptance angle $\phi=15$ mrad.

RESULTS AND DISCUSSION

A Round Robin Test (RRT) has been carried out on different solar reflector materials: a commercial 2 mm silvered-glass mirror, an aluminum mirror with several thin PVD layers to enhance reflectance, a silvered-polymer mirror and a 4 mm silvered-glass mirror with a prototype anti-soiling coating on top of the glass.

Hemispherical Reflectance

Hemispherical reflectance was measured at near normal incidence angles with spectrophotometers. DLR/CIEMAT and ENEA used commercial spectrophotometers from Perkin Elmer (models Lambda 1050 and 950 respectively) with an integrating sphere of 150mm in diameter. Fraunhofer used a Bruker IFS 66 spectrophotometer with an integrating sphere of 200mm. UNIZA used the laboratory setup described in the previous section. The weighting with the obtained reflectance spectrum was performed with the direct normal Air Mass 1.5 ASTM G173 reference spectrum. FIGURE 5 shows the obtained results.

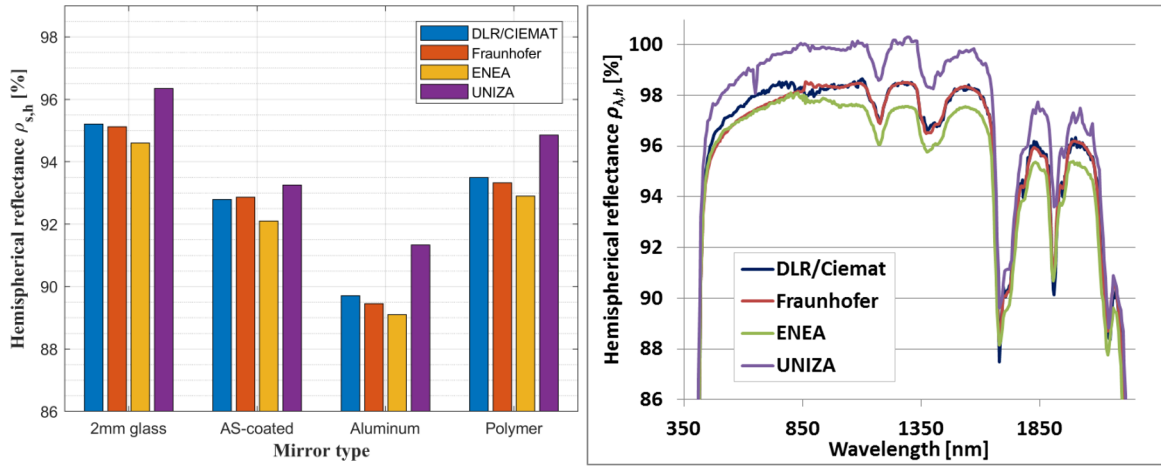


FIGURE 5. Round Robin test results a) solar weighted hemispherical reflectance, uncertainty of all equipment is $\sim 0.7\%$ -p. b) measured hemispherical spectra of the silvered-polymer mirror

Good agreement was achieved in terms of the solar weighted hemispherical reflectance $\rho_{s,h}$ for the commercial spectrophotometers with a maximum standard deviation of $\sigma=0.34\%$ -p among the labs DLR/CIEMAT, Fraunhofer and ENEA. The measured values from UNIZA are systematically higher in the range of 0.7 to 1.9%-p (see FIGURE 5a). This effect is also visible when comparing the hemispherical reflectance spectra (as example, the spectra of the silvered-polymer mirror is shown in FIGURE 5b).

Near-Specular Reflectance

The near-specular reflectance was evaluated with the four newly developed instruments described in the previous section. ENEA evaluated the measured data with two different models: the traditional independent EMA and TIS, as well as an improved model, in which EMA and TIS are coupled as described below. All samples have been measured at $\theta_i=10, 30$ and 60° and at $\varphi=15\text{mrad}$, with a beam divergence of $\varphi_s=4.7\text{mrad}$. Thus, all values are expressed in terms of sun-conic reflectance $\rho_{s,\varphi,\varphi_s}$. The solar weighting was performed with the direct normal Air Mass 1.5 ASTM G173 reference spectrum.

FIGURE 6 shows $\rho_{s,\varphi,\varphi_s}$ of the different instruments for the 4 mirror types measured. For the case of the 2mm silvered-glass mirror the lowest standard deviations among the laboratories are appreciated ($\sigma=0.48\%$ -p). Thus, a slightly lower agreement as for the hemispherical RRT is achieved. The silvered-glass mirror shows constant reflectance values over the range $\theta_i=[10-60]^\circ$. The measurement results of the 4mm silvered-glass mirror with anti-soiling coating show slightly higher standard deviations among the laboratories of $\sigma=0.54\%$ -p. The highest deviations of $\sigma=1.99\%$ -p are observed for the aluminum mirror. A systemically lower reflectance was measured by DLR/CIEMAT compared to the rest of partners. Intermediate standard deviations up to $\sigma=0.78\%$ -p were obtained for the polymer mirror.

The experimental methods of DLR/CIEMAT, Fraunhofer and UNIZA all indicate decreasing reflectance behavior with growing θ_i for the measured samples, except for the 2mm silvered-glass mirror, which is independent of θ_i . Opposite to this agreement, the ENEA approach, which is based on monochromatic measurements and modelling, indicates an increase of sun-conic reflectance with growing θ_i . Although the improved EMA-TIS model

by ENEA results in smaller deviations at large θ_i , further optimization is ongoing to converge with the experimental findings.

FIGURE 7a shows a comparison between the specular and sun-conic reflectance for the polymer mirror, measured by ENEA and Fraunhofer. It is possible to see that the sun-conic reflectance is lower than the specular reflectance in any case. While the differences decrease for smaller acceptance angles for the Fraunhofer results (shown in green), they increase for the ENEA results (shown in blue). Also an opposite angular concerning behavior was measured by both institutes. The deviations are still under investigation.

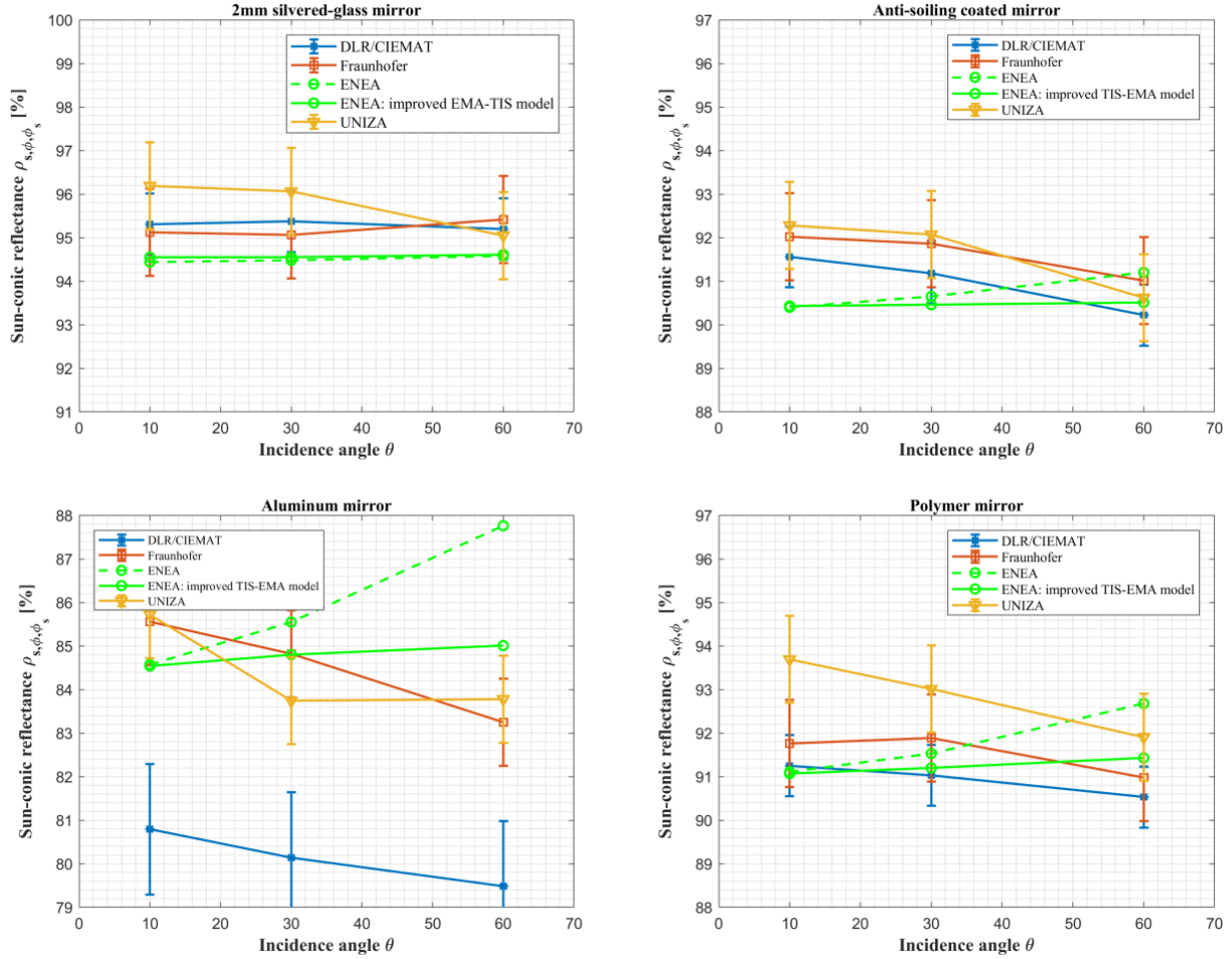


FIGURE 6. Round Robin test results in terms of solar-weighted sun-conic reflectance ρ_{s,ϕ,ϕ_s} at different incidence angles for the four different mirror types. Note that the y-axis shows different scales but the interval is 9 %-p for every graph.

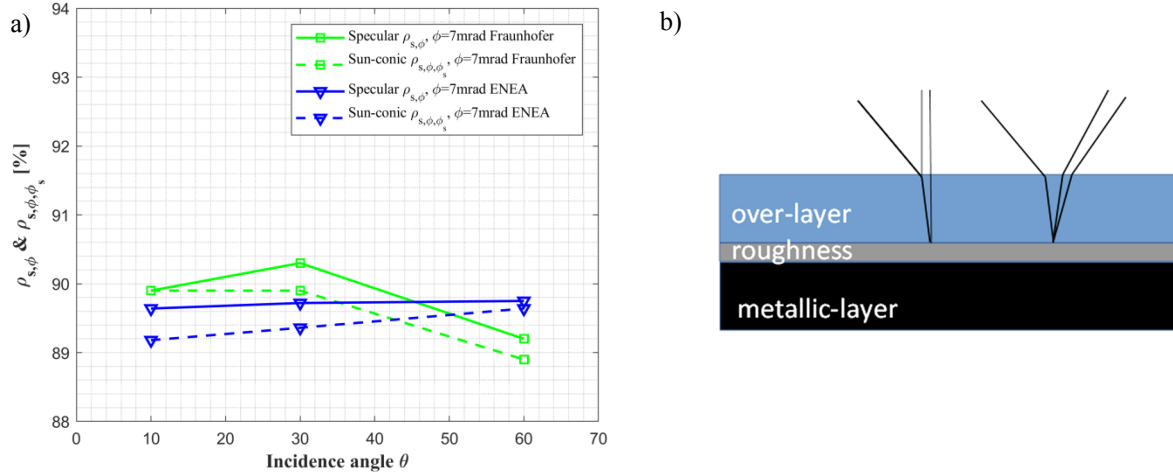


FIGURE 7. a) Comparison of sun-conic and specular reflectance at 7 mrad for the polymer mirror at different θ_i . b) visualization of improved EMA-TIS modelling approach by ENEA, taking into account changes in incidence (left rays) and acceptance angle (right rays) due to refraction at the over-layer.

As discussed above, the results from FIGURE 6 show similar angular behavior between the DLR/CIEMAT, Fraunhofer and UNIZA measurements, while opposite angular behavior is detected by SMQ2 from ENEA. As a matter of fact, DLR/CIEMAT, Fraunhofer and UNIZA accomplish the measurements at the specific incidence angle of interest. Differently, the ENEA approach is based on hemispherical and SMQ2 measurements accomplished at near-normal incidence. Then the off-normal hemispherical spectra are predicted by EMA, and multiplied by the TIS_E -factor, in which the equivalent roughness σ_ϕ was measured by SMQ2, to obtain off-normal near-specular reflectance spectra.

$$\frac{\rho_{\lambda,\phi}(\lambda, \theta_i, \phi)}{\rho_{\lambda,h}(\lambda, \theta_i, \phi)} = \exp \left[- \left(\frac{4\pi\sigma_\phi \cos(\theta_i)}{\lambda} \right)^2 \right] = TIS_E \quad (1)$$

The comparison indicates that EMA-TIS modeling, as initially conceived, fails to fit the angular behavior of the most diffusive specimens. That disagreement has led to improve the EMA-TIS model, by more properly pinpointing the scattering at the internal interface between metallic surface and protective transparent over-layer of the equivalent model used in EMA (see FIGURE 7b). As a consequence, in the new approach TIS and EMA are merged one into each other; in the case of near-specular computing the reflectance at the interface over-layer|metallic-layer is attenuated by the modified TIS_{E*} factor:

$$TIS_{E*} = \exp \left[- \left(\frac{4\pi\sigma_{\phi_{ol}} \cos(\theta_{ol})}{\lambda/n_{ol}} \right)^2 \right] \quad (2)$$

where the “ol” index indicates that the quantity refers to the over-layer; in particular $\theta_{ol} = \arcsin \left(\frac{\sin(\theta_i)}{n_{ol}} \right)$. In the case of hemispherical reflectance, the reflectance at the interface over-layer|metallic-layer is integrally considered.

Noteworthy, now the equivalent roughness $\sigma_{\phi_{ol}}$ is driven by the acceptance angle in the over-layer, ϕ_{ol} , which is related to the one in air, ϕ , according to the sine’s law. The acceptance angle ϕ_{ol} decreases with increasing incidence angle θ_i . This is the main reason for the observed decreasing behavior of the near-specular reflectance versus the incidence angle for the most diffusive specimens. The new coupled EMA-TIS model fits quite well the experimental data got with the others instruments, although further research is being conducted to refine the model (e.g. improving off-normal prediction of hemispherical reflectance by including the effect of trapped light between metallic and over-layer at higher θ_{ol}).

Since Fraunhofer’s VLABS only measures at discrete wavelengths, the TIS -theory proposed by ENEA is applied to obtain spectral behavior. However, in difference to ENEA, near-specular measurements can be carried out also at off-normal θ_i . The initially proposed TIS-model (see eq.1 and [6]) has been adapted in [9], where an additional equivalent incidence angle factor ε is introduced, considering the multiple optical layers.

$$\frac{\rho_{\lambda,\varphi}(\lambda, \theta_i, \varphi)}{\rho_{\lambda,h}(\lambda, \theta_i, \varphi)} = \exp \left[- \left(\frac{4\pi\sigma_\varphi \cos(\theta_i \varepsilon)}{\lambda} \right)^2 \right] = TIS_F \quad (3)$$

In contrast to the above described methods, the measurements from DLR/CIEMAT and UNIZA do not require any modelling, since near-specular reflectance is directly measured for the λ -, θ_i - and φ of interest.

SUMMARY

In order to extend the characterization of solar-weighted near-specular reflectance towards off-normal behavior, four experimental reflectometers of different research organizations have been improved. A Round Robin Test with four different mirror types has been conducted at $\theta_i = 10, 30$ and 60° and at $\varphi = 15$ mrad. The beam divergence of all reflectometers was set to $\varphi_s = 4.7$ mrad, simulating the sun disc at clear sky conditions. Fraunhofer and ENEA applied different Total Integrated Scatter models to compute spectral data based on measurements at discrete wavelengths. DLR/CIEMAT and UNIZA directly measured the reflectance spectrum in the wavelength range of 320-2500 nm. The obtained results among the laboratories showed good agreement for the silvered-glass mirror. This mirror type exhibited constant reflectance properties up to 60° of incidence and it can be concluded that near-normal measurement as indicated in the SolarPACES reflectance guideline is sufficient for silvered-glass mirrors. However, decreasing reflectance with incidence angle was measured by DLR/CIEMAT, Fraunhofer and UNIZA for the glass mirror with anti-soiling coating, the polymer- and especially the aluminum mirror specimens. As a consequence, ENEA's model to predict off-normal behavior was improved. For latter mentioned mirror types, off-normal behavior needs to be considered if accurate estimations of the annually reflected solar energy towards the receiver want to be obtained. The highest deviation among laboratories were found for the aluminum-, followed by the anti-soiling coated-, the polymer- and finally the glass mirror.

NOMENCLATURE

<i>EMA</i>	Equivalent Model Algorithm
<i>TIS_E</i>	Total integrated scatter-factor applied by ENEA to compute near-specular spectral reflectance
<i>TIS_E*</i>	Improved <i>TIS_E</i> -factor applied by ENEA to compute near-specular spectral reflectance
<i>TIS_F</i>	Total integrated scatter-factor applied by Fraunhofer to compute near-specular spectral reflectance
ε	equivalent incidence angle factor
θ_i	incidence angle in $^\circ$
θ_{ol}	incidence angle within the over-layer in $^\circ$
λ	wavelength in nm
$\rho_{s,h}$	solar-weighted hemispherical reflectance in the range $\lambda = [300-2500]$ nm at $\theta_i = 8^\circ$
$\rho_{s,\varphi,\varphi_s}$	sun-conic solar-weighted reflectance in the range $\lambda = [300-2500]$ nm and at $\varphi = 15$ mrad
$\rho_{\lambda,h}$	spectral hemispherical reflectance at wavelength λ . For the measurements in this paper: $\theta_i = 8^\circ$
$\rho_{\lambda,\varphi}$	specular reflectance at wavelength λ , incidence angle θ_i and acceptance angle φ
σ	standard deviation
σ_φ	equivalent roughness
$\sigma_{\varphi ol}$	equivalent roughness in over-layer
φ	acceptance half-angle in mrad related to the mirror scattering. Here $\varphi = 15$ mrad.
φ_{ol}	acceptance half-angle in mrad within the over-layer
φ_p	acceptance half-angle in mrad related to the mirror shape inaccuracies.
φ_r	acceptance half-angle of the solar receiver in mrad.
φ_s	beam divergence of sun or the light source in the reflectometer in mrad. Here $\varphi_s = 4.7$ mrad.
φ_t	acceptance half-angle in mrad related to the mirror tracking inaccuracies.

ACKNOWLEDGEMENTS

The research conducting to the results of this paper were funded by SolarPACES within the project “Measuring and modelling near-specular solar reflectance at different incidence angles”.

REFERENCES

1. F. Sutter, M. Montecchi, H. von Dahlen, A. Fernández-García, M. Röger: The effect of incidence angle on the reflectance of solar mirrors. [Solar Energy Materials and Solar Cells](#) 176 (2018) 119-133
2. A. Rabl: Comparison of Solar Concentrators. [Solar Energy](#), Vol. 18, pp. 93-111, Pergamon Press 1976.
3. M. Montecchi.: Proposal of a New Parameter for the Comprehensive Qualification of Solar Mirrors for CSP Applications. [AIP Conference Proceedings](#) 1734, 130014 (2016); doi: 10.1063/1.4949224
4. SolarPACES Reflectance Guideline, Version 3.0. March 2018. http://www.solarpaces.org/wp-content/uploads/20180320_SolarPACES-Reflectance-Guidelines-V3.pdf
5. F. Sutter, S. Meyen, A. Fernandez-García, P. Heller: Spectral characterization of specular reflectance of solar mirrors. [Solar Energy Materials & Solar Cells](#) 145 (2016) 248-254.
6. M. Montecchi, “Approximated method for modelling hemispherical reflectance and evaluating near-specular reflectance of CSP mirrors”, [Solar Energy](#) 92 (2013) 280-287.
7. P. Beckman and A. Spizzichino, “The scattering of electromagnetic waves from rough surfaces”, Pergamon/Macmillan 1963.
8. A. Heimsath, T. Schmid, P. Nitz. “Angle resolved specular reflectance measured with VLABS”. [Energy Procedia](#) 69 (2015) 1895 – 1903.
9. A.Heimsath, P.Nitz “Scattering and specular reflection of solar reflector materials – measurements with VLABS and method for solar weighted specular reflectance”, to be published
10. M. Montecchi, “Upgrading of ENEA solar mirror qualification set-up”, [Energy Procedia](#) 49 (2014) 2154-216; doi: 10.1016/j.egypro.2014.03.228.